International Journal of Power Electronics and Drive Systems (IJPEDS)
Vol. 16, No. 1, March 2025, pp. 642~656
ISSN: 2088-8694, DOI: 10.11591/ijpeds.v16.i1.pp642-656

Development of random pulse width modulation technique for voltage source inverter drives

Quoc Dat Luong[1,2], Manh Duc Nguyen[1,2], Minh Khoi Huynh[1,2], Phu Cong Nguyen[1,2,3], Quoc Dung Phan[1,2]
[1]Faculty of Electrical and Electronics Engineering, Ho Chi Minh City University of Technology, Ho Chi Minh City, Vietnam
[2]Vietnam National University Ho Chi Minh City (VNU-HCM), Ho Chi Minh City, Vietnam
[3]Department of Electrical and Electronics Engineering, Ho Chi Minh City University of Industry and Trade, Ho Chi Minh City, Vietnam

Article Info

Article history:

Received May 22, 2024
Revised Nov 18, 2024
Accepted Nov 28, 2024

Keywords:

EMI
Genetic algorithm
Optimization
Random PWM
THD

ABSTRACT

In this research, the structure selection of the carriers in the implementation of random pulse width modulation (RPWM) method for single-phase voltage source inverter (VSI) drives is specified by a 16-bit binary sequence. Subsequently, the genetic algorithm (GA) is used to find the solution of the optimal sequence allowing the output voltage signal to achieve the minimum total harmonic distortion (THD). In addition, the harmonic spreading factor (HSF) is further analyzed to evaluate the acoustic noise and electromagnetic interference (EMI) of the operation of electromechanical system. Finally, through hardware testing process, the simulation results are validated in order to ensure the reliability of our research findings. The main components of this testing process are LAUNCHXL-F28379D utilized to generate controlling pulses for the modules insulated gate bipolar transistors (IGBT), and two EVAL-1EDI60I12AF gate driver modules for realizing the full-bridge inverter.

Corresponding Author:

Quoc Dung Phan
Faculty of Electrical and Electronics Engineering, Ho Chi Minh City University of Technology
268 Ly Thuong Kiet Street, District 10, Ho Chi Minh City 700000, Vietnam
Email: pqdung@hcmut.edu.vn

1. INTRODUCTION

In contemporary applications, the conventional sinusoidal pulse width modulation (SPWM) control technique is prevalently utilized for motor control. However, it engenders a degradation in voltage quality after modulation, attributable to the emergence of substantial harmonic amplitudes in proximity to the switching frequency. This phenomenon precipitates audible mechanical noise, vibrations, and electromagnetic interference during the operation of electromechanical systems [1]. A plethora of solutions to mitigate this issue have been proposed by various researchers in preceding studies. The article [1], [2] presented the random carrier PWM (RCPWM) method using pseudo-random bit sequence (PRBS). The random reference PWM (RR-PWM) and random reference and random carrier PWM (RRRC-PWM) method with the randomness introduced in both generation of modulating signal and selection of carrier signal were mentioned in the [3]. Nayeemuddin *et al.* [4] discusses the implementation of random modulating-carrier PWM algorithm for cascaded multilevel inverter fed induction motor drive. The encoding of a random carrier as a gene, the random carrier sequence corresponding to a chromosome, and the fitness function as the reciprocal of the maximum amplitude of the harmonic spectrum for RCPWM based on the genetic algorithm described were proposed in [5]. Others strategies involve the utilization of randomized carrier frequency modulation (RCFM) [6]-[8], chaotic carrier random pulse width modulation (CCRPWM) [9] and randomized pulse position modulation (RPPM) as well as the dual RPWM methodology, which amalgamates the RCFM and RPPM schemes, is also applied in [8]. Besides that, the implementation of the random space vector pulse width modulation (RSVPWM) technique is frequently employed as an efficacious solution for the generation of a randomness carrier [10]-[14]. Furthermore, the RPWM algorithm can also be applied in photovoltaic (PV) inverter systems for domestic utilization [15].

In the present study, a novel approach for the development of RPWM technique employed in single-phase voltage source inverter (VSI) will be investigated. The configuration of carrier structures in this technique is characterized by a 16-bit binary sequence. Two different methods for carrier regulation are proposed in relation to the algorithm mentioned above. Subsequently, the genetic algorithm (GA) is applied to determine the optimal binary sequence solution, thereby allowing the output voltage signal to attain the minimum total harmonic distortion (THD). A comprehensive analysis of the harmonic spectrum structure of the output voltage signal is also conducted through the calculation of the HSF.

2. THE PROPOSED RPWM TECHNIQUES

Within the framework of the RPWM technique, the sinusoidal alternating current (AC) reference voltage signal is compared with the high-frequency random triangular carrier signal in a real-time setting. This comparison is instrumental in ascertaining the switching states for the gates of the IGBT power modules within single-phase VSI. Furthermore, the level-shifted approach is selected as the modulation scheme within this technique. Afterward, the continuous triangular carriers corresponding to each randomly generated binary bit value are constructed. This allows for the carrier shape to dynamically adapt to instantaneous binary values, thereby reducing THD in comparison to the conventional SPWM also known as fixed-frequency PWM control. Thus, the simulation experiments of the RPWM are carried out through two distinct alternatives:

- + Option 1: Binary bit values of 0 and 1 are respectively assigned to the lower and upper waveforms, both exhibiting identical frequency *f* and amplitude A.
- + Option 2 is construed as an extension of the waveforms established in option 1: A binary bit value of 0 designates the “small” waveform (with a frequency 2*f* and amplitude A), while a binary bit value of 1 designates the “large” waveform (with a frequency f and amplitude 2 A).

Employing values where the amplitude A is set to 0.25 and the frequency *f* is established at 8 kHz (8 kHz is not too high to avoid generating excessive thermal losses in the semiconductor switches during the operation of this inverter). The frequency of the reference sinusoidal wave is determined to be 50 Hz. Consequently, the retention duration for each single bit in the binary sequence is calculated as 0.02/16, equating to 0.00125 seconds. The cumulative duration for each binary sequence is determined to be 1/50, or 0.02 seconds. This data serves as a representative sample for our research. In reality, the algorithm can be extended to accommodate 8-bit, 32-bit, or 64-bit configurations, and the frequency of the carrier wave can be increased to facilitate the modulation of voltage in metal-oxide-semiconductor field-effect transistor (MOSFET) modules.

In these 2 proposed options, a systematic shift of binary digits within a 16-bit sequence is performed for transitioning into the processor from the least significant bit (LSB) to the most significant bit (MSB). This process is instrumental in controlling the selection of carriers, as shown in Figures 1 and 2 (see Appendices). Subsequently, this specific 16-bit sequence is reiterated in the ensuing cycles of the reference sinusoidal wave. Each carrier signal is then compared with the reference signal to generate 2 switching signals which are complementary for controlling 1 leg of the VSI.

In addition to the existing configuration, it is possible to create segments exhibiting a holding state into the centroid of the selected waveform in the retention duration for each single bit in the binary sequence, as shown in Figure 3 (see Appendices). This approach reduces the number of switching times per cycle of the reference sinusoidal wave, thereby reducing switching losses on semiconductor switches and enhancing the efficiency of the overall system. Nevertheless, the applications of this proposal in the domain of electromechanical system control present challenges due to the non-linear characteristics of the system properties. Moreover, this non-linearity complicates the system’s response and behavior, thus posing difficulties in controlling them effectively. Hence, in the following sections of this research, our primary focus will be to meticulously analyze the characteristics of the 2 modulation techniques shown in Figures 1 and 2.

3. RESEARCH METHOD-OPTIMIZATION OF OUTPUT VOLTAGE THD IN RANDOM MODULATION SCHEMES

In this section, the application of GA [16], [17] is employed to determine the optimal bit sequence crucial for controlling the carrier signal that modulates the output voltage. Through the optimization of the bit sequence, the attainment of an output voltage with minimal THD is effectively facilitated. The algorithm flowchart presented in Figure 4 describes the evolution process of the natural population with *N* being the number of individuals in the population, through the processes of generate population, fitness evaluation, selection, crossover, mutation, replacement, and termination check. each of these individuals is a 16-bit binary string that characterizes the configuration of carrier structure to regulate the output voltage.

The fitness function is utilized to assess the quality or suitability of individuals within a population [18]. This assessment is pivotal in determining the reproductive success of each individual, which is inherently proportional to their fitness. In this research, our fitness function is THD of the output voltage calculated up to 30 kHz as shown in (1).

$$THD = \sqrt{\frac{\sum_{n=2}^{600} H_n}{H_1}} \tag{1}$$

Where, H_n is the amplitude of the n^{th} harmonic voltage. Notably, our methodology allows for a comprehensive extension of the calculated frequency range to even higher frequencies. This capability enhances the scope providing a more versatile analytical framework.

In this research, the method of real number encoding [19], [20] is applied to determine the optimal 16-bit sequence that regulates the output voltage with minimal THD. Notably, the real-encoded values of 16-bit sequences are discrete integers within the range of 0 to 2^{16}-1 = 65535. This characteristic significantly enhances the efficiency of the GA in identifying the optimal solution, thereby accelerating the overall computational process.

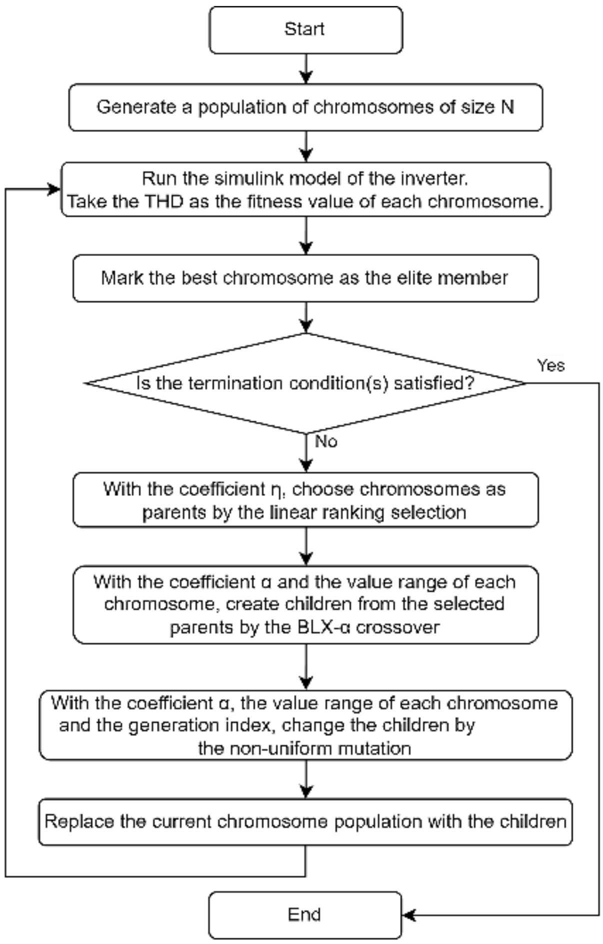

Figure 4. The procedure of our proposed GA

The linear ranking selection [21]-[23] is also applied in our algorithm to eliminate some individuals with lower adaptability, leading to a reduction in genetic diversity in the population and, as a result, earlier convergence of the minimal THD. In the process of optimizing adaptability, individuals are systematically organized in an ascending sequence. The individual exhibiting the highest performance is conferred with the rank of *N*, while the one demonstrating the least performance is assigned the rank of 1. It is noteworthy that the probability of selection for each individual is directly commensurate with its respective rank [24]. The selection probability of each individual is directly proportional to its rank as shown in (2).

$$p_k = \frac{1}{N}\left[\eta + 2(1-\eta)\frac{k-1}{N-1}\right] \quad (2)$$

Where, $k = \overline{1..N}$ and $0 < \eta < 1$.

In addition, non-uniform mutation is used in GA to randomly alter one or more genes of each individual to increase structural diversity within the population. The mutation operation guarantees a non-zero probability of reaching any point in the search space. We defined $s_v^t = \langle v_1 \dots v_m \rangle$ is a chromosome (t is the generation number) and the element v_k was selected for this mutation, the result is a vector $s_v^{t+1} = \langle v_1' \dots v_k' \dots v_m' \rangle$, with v_k' calculated according to (3).

$$v_k' = \begin{cases} v_k + \Delta(t, UB - v_k) & \text{if a random digit is 0} \\ v_k - \Delta(t, v_k - LB) & \text{if a random digit is 1} \end{cases} \quad (3)$$

Where LB and UB are lower and upper domain bounds of the variable v_k [25]. The function $\Delta(t, y)$ returns *a* value in the range $[0, y]$ such that the probability of $\Delta(t, y)$ being close to 0 increases as t increases. The $\Delta(t, y)$ function is defined by the mathematical expression as shown in (4).

$$\Delta(t, y) = y \times \left[1 - r^{\left(1-\frac{t}{T}\right)^b}\right] \quad (4)$$

Where r is a random number in the range [0,1], T is the maximal generation number, and b is a system parameter determining the degree of dependency on iteration number [25]. The non-uniform mutation proves particularly well-suited for real-coded GA owing to its inherent characteristic wherein the influence of the mutation process diminishes over an extended runtime of the GA [26].

Finally, the blend crossover (BLX-α) technique [27]-[29] is applied as a GA-based method in exploring the search space by generating offspring's that are a blend of the parent genes and optimizing complex multi-modal functions. The gene c_k of the offspring chromosome is randomly selected within the closed interval $[\underline{c}_k, \bar{c}_k]$ as represented in (5).

$$c_k = \text{random}([\underline{c}_k, \bar{c}_k]) \text{ with } \underline{c}_k = \min(a_k, b_k) - \alpha\|a_k - b_k\| \text{ and}$$
$$\bar{c}_k = \max(a_k, b_k) + \alpha\|a_k - b_k\| \quad (5)$$

The BLX-α crossover operation (especially in the case of $\alpha = 0.5$) and linear crossover are most suitable for real-encoded GA. These operations have the ability to generate offspring outside the domain $[\min(a_k, b_k), \max(a_k, b_k)]$ ensuring no potential solutions overlooked during the search process [29].

4. RESULTS AND DISCUSSION

In this section, we apply the computational capabilities of MATLAB in conjunction with the PLECS BLOCKSET packages. These tools are utilized to execute the GA in order to identify the optimal 16-bit sequence. The model of power converter built in the PLECS BLOCKSET is described in Figure 5 and the initial parameters of GA on MATLAB are described in Table 1.

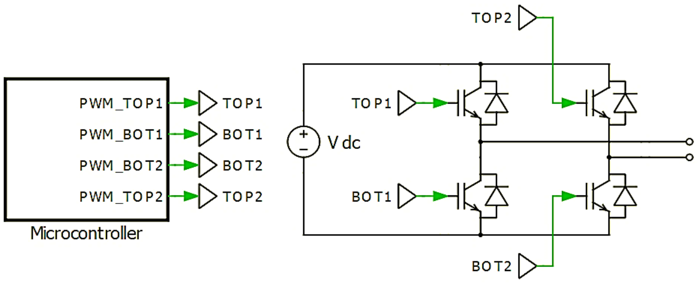

Figure 5. The topology of a single-phase H-bridge VSI

After successfully executing GA, the optimal 16-bit sequence of option 1 and option 2 is acquired as 0111 1111 1000 0000 (the equivalent real-coded value is 32640) and 0011 1100 0000 0000 (the equivalent real-coded value is 15360) respectively. The results of searching for individual with the optimal THD according to each generation of GA are shown in Figure 6. With a modulation index of 0.8, the optimal bit sequence for option 1 is discovered in the 18th generation where the corresponding THD values of the output voltage are 28.8196% (considering the highest harmonic frequency of 30 kHz) and 29.5373% (considering the Nyquist frequency of 500 kHz). Similarly, for option 2, the optimal bit sequence is discovered in the 17th generation where the corresponding THD values of the output voltage are 44.66% (considering the highest harmonic frequency of 30 kHz) and 48.51% (considering the Nyquist frequency of 500 kHz). The rate of convergence is remarkably swift and by running a maximum of 80 generations on a total of 65536 cases (which constitutes a mere 0.122% of the search space), we successfully determine the optimal 16-bit sequence. Given this rapid convergence, we can confidently extend the application of GA in order to find the optimal 32-bit or 64-bit binary sequence with similarly efficient rate of convergence. We will then proceed to compare the performance of these optimal 16-bit sequences with 2 specific random 16-bit sequences.

Table 1. Genetic algorithm parameters

Parameters	Values	Parameters	Values
Population-size	10	Sequence-bit	16
Max-generations	80	α-crossover	0.5
Max-stall-generations *(the maximum number of generations which the GA can take)*	75	*b*- mutation	5
Range	[1 65535]	DC-voltage-supply	200 V

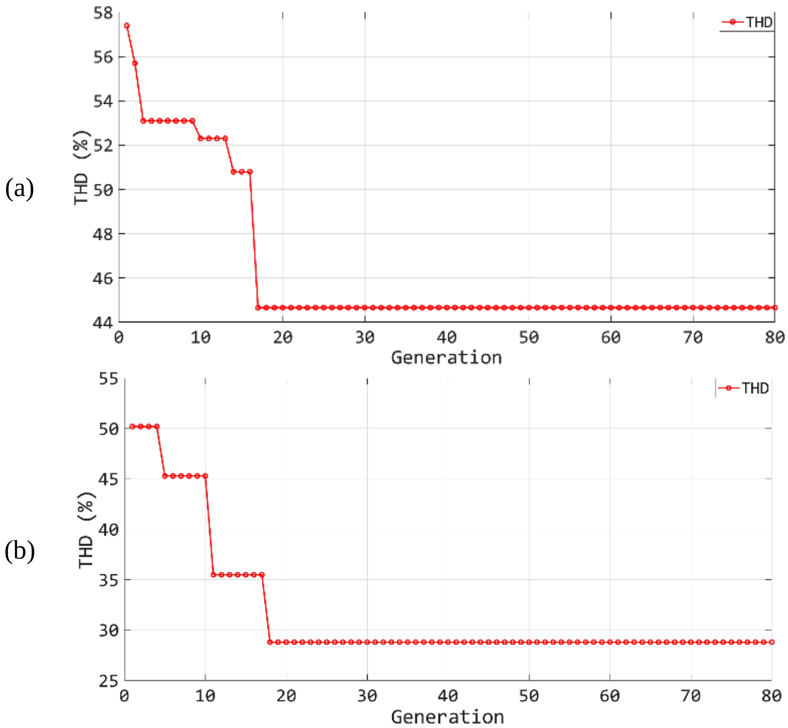

Figure 6. The statistical results of the best suited individual within the population in each generation: (a) the option 1 and (b) the option 2

4.1. Simulation results on PLECS software

4.1.1. The option 1

The simulation results of analyzing the output waveform of the optimal sequence and the sequence with the equivalent real-coded value of 65027 (arbitrary value) with a modulation index of 0.8 are shown in Figures 7 and 8, respectively. In Figure 7, the HSF and THD values of the harmonic spectrum are 4.9486 and 29.5373%, respectively. Meanwhile, in Figure 8, these HSF and THD values are 5.2289 and 31.3598%, respectively, with HSF is determined by (6).

$$HSF = \sqrt{\frac{\sum_{n=2}^{600}(H_n - H_0)^2}{600}} \quad (6)$$

Where, $H_0 = \sum_{n=2}^{600} H_n / 600$ and HSF measures the effectiveness of suppressing dominant harmonics.

The harmonic spectrum defined by the optimal sequence has better quality than the harmonic spectrum defined by the sequence with the arbitrary value as the ripple in the harmonic spectrum evaluated by HSF is smaller (4.9486<5.2289). The THD value is lower (29.5373%<31.3598%). Thus, the optimal random method significantly reduces acoustic noise caused by harmonics during operation.

(a)
(b)
(c)

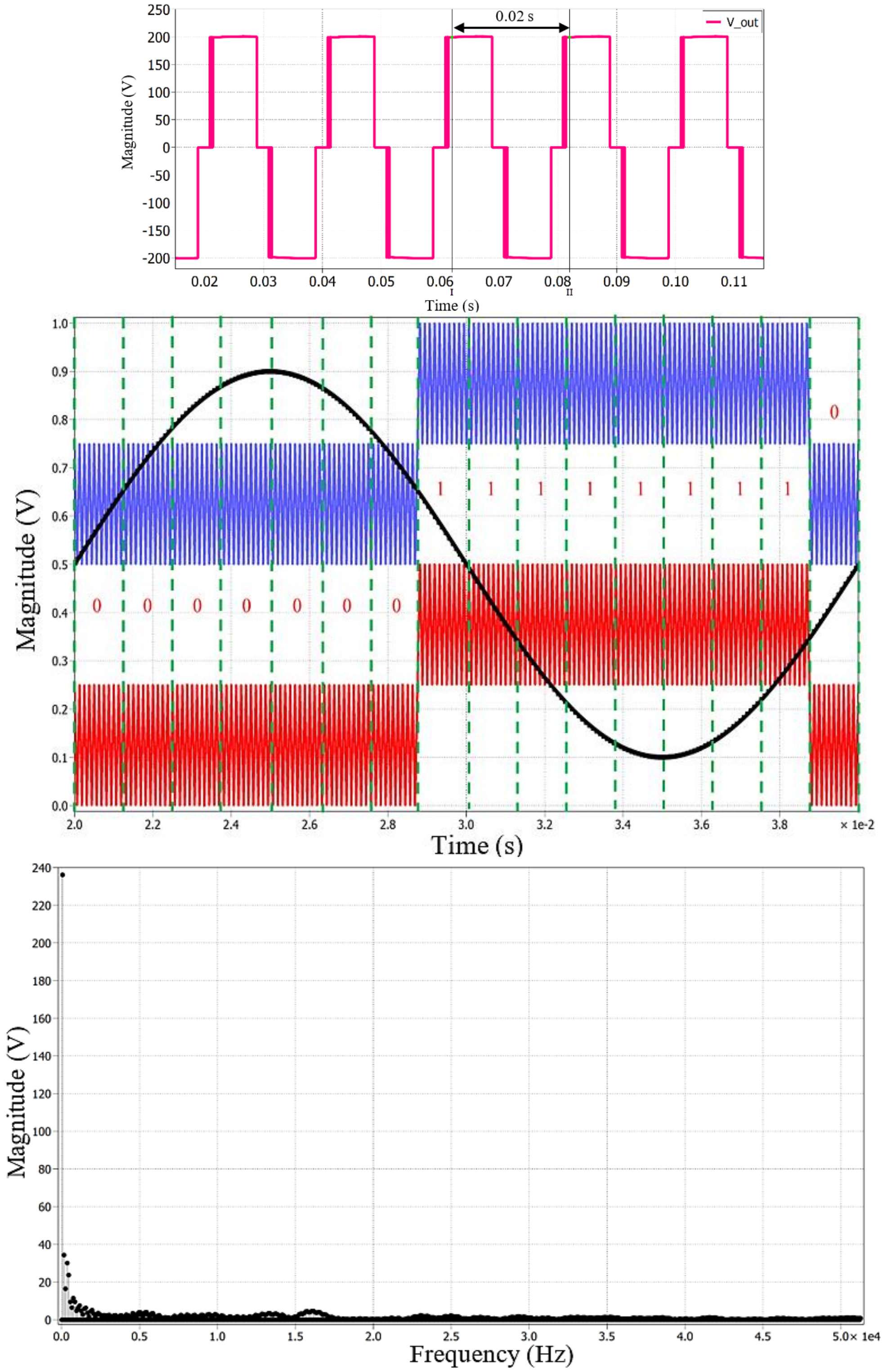

Figure 7. Results obtained of the output voltage delineated by the optimal sequence: (a) the corresponding output voltage waveform, (b) the reference sinusoidal waveform and the carrier waveform, and (c) the harmonic spectrum

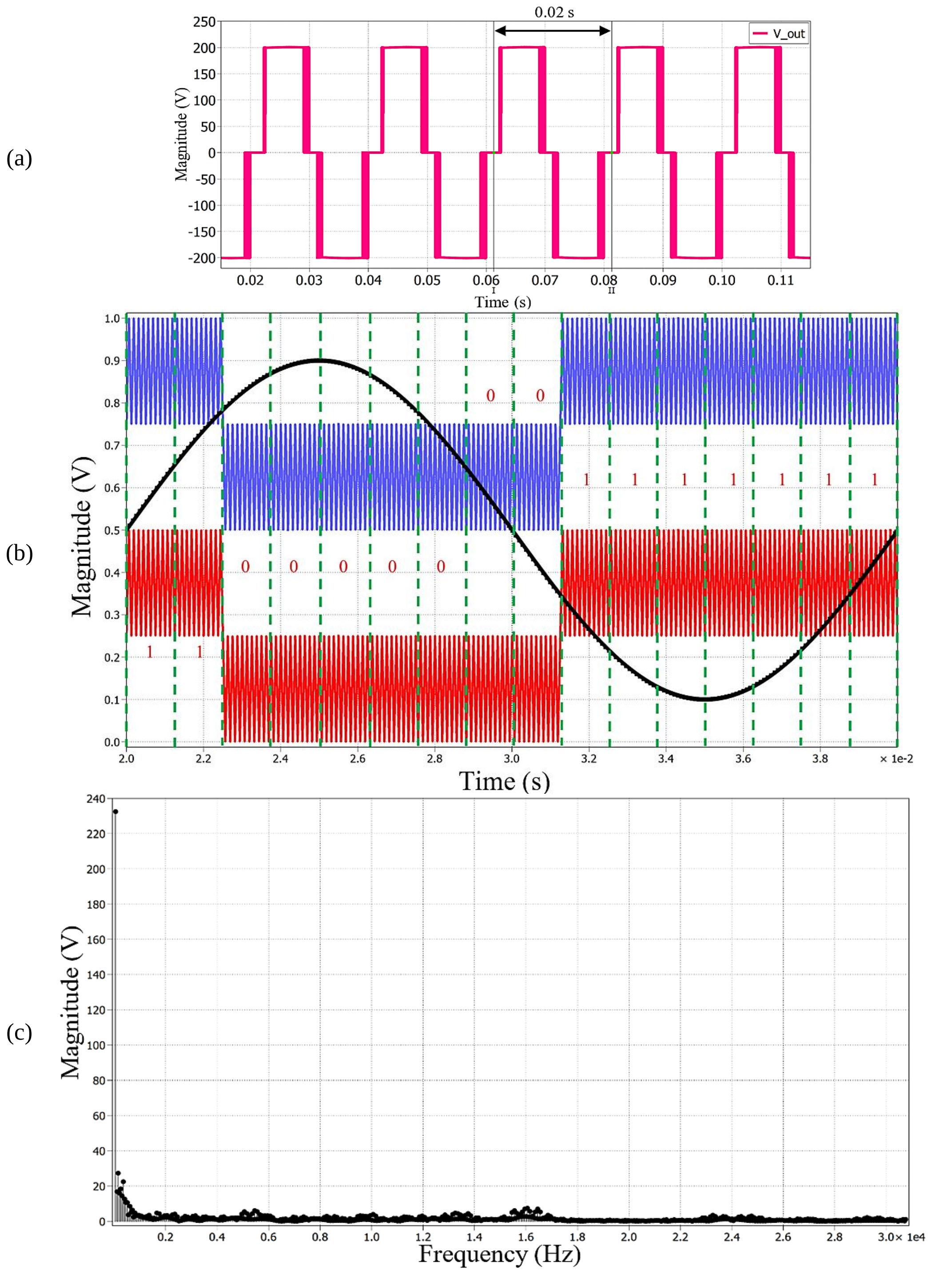

Figure 8. Results obtained of the output voltage delineated by the sequence with the equivalent real-coded value of 65027: (a) the corresponding output voltage waveform, (b) the reference sinusoidal waveform and the carrier waveform, and (c) the harmonic spectrum

4.1.2. The option 2

The simulation results of analyzing the output waveform of the optimal sequence with a modulation index of 0.8 are shown in Figure 9. In Figure 9, the HSF and THD values of the harmonic spectrum are 10.5399 and 48.5071%, respectively. Option 2 does not provide the same effectiveness in reducing acoustic noise as option 1, because significant harmonics appear in the harmonic spectrum at frequencies of 8 kHz and 16 kHz. Thus, this modulation method is not suitable, even though the THD value after optimization by GA is lower than that of the fixed-frequency method.

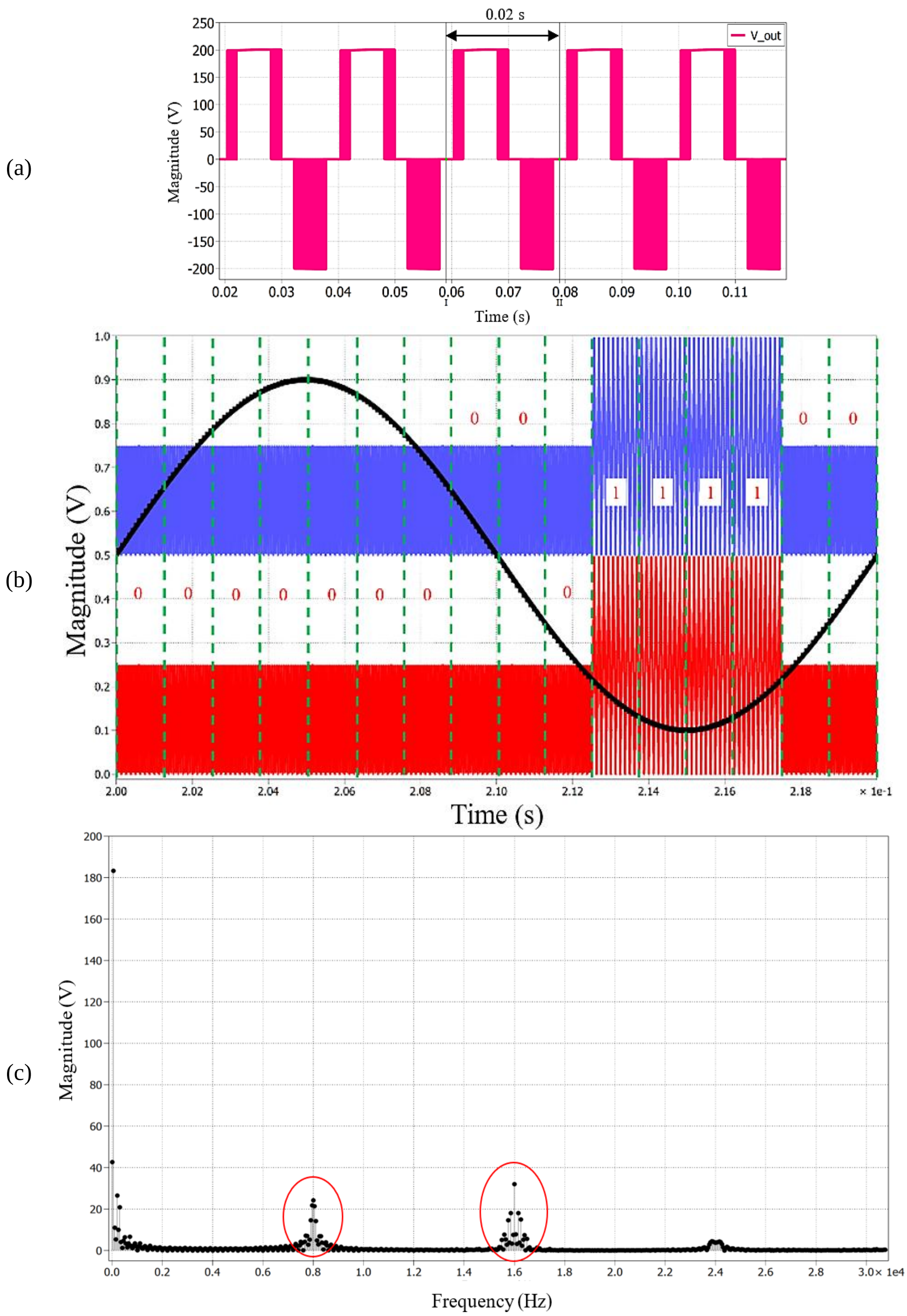

Figure 9. Results obtained of the output voltage delineated by the optimal sequence: (a) the corresponding output voltage waveform, (b) the reference sinusoidal waveform and the carrier waveform, and (c) the harmonic spectrum

4.1.3. Discussion

The graph describing the variation of THD and HSF, as influenced by the modulation index (MI), is shown in Figures 10 and 11. GA-optimized RPWM exhibits lower THD compared to conventional RPWM and achieves better HSF, indicating improved harmonic suppression. Option 1 surpasses option 2 because there are no dominant harmonics in the high-frequency region in option 1. The output voltage waveform of option 1 is symmetrical about the horizontal axis and this symmetrical waveform characteristic ensures that zero-order harmonics (also known as DC components) are negligible in the harmonic spectrum. Actually, DC components can saturate in power transformers and it can cause vibration and audible noise in transformers. Thus, in the hardware experiments intended to validate the efficacy of this research, the RPWM method is exclusively implemented by using the option 1.

For the reasons above, the algorithm of option 1 can be completely applied to modulate three-phase voltage for the control of AC motors. Subsequently, a speed control model specifically designed for squirrel-cage induction motors is also proposed. Specifically, this model utilizes a three-phase VSI, modulated by GA-optimized RPWM, with the input power for this system sourced from the solar panel system. This is one of the important applications of this algorithm for self-consumption of PV renewable energy.

4.2. Hardware experiments

The hardware experiment utilized to validate the developed control method is shown in Figure 12. The LAUNCHXL-F28379D Development Kit generates control signals PWM_TOP1 and PWM_BOT1 through pins J4-40 (GPIO0) and J4-39 (GPIO1), and PWM_TOP2 and PWM_BOT2 through pins J4-38 (GPIO2) and J4-37 (GPIO3), supplying two EVAL-1EDI60I12AF modules via X1-B7 and X1-B8. The F28379D Kit also generates GND signals through J2-20 and J10-GND for the 1EDI60I12AF modules via the RESET Signal GND pin, provides a 3.3V ENABLE voltage through J1-1 and J5-41 via X1-B3, and a GND voltage through J7-62 and J10-GND via X1-A16.

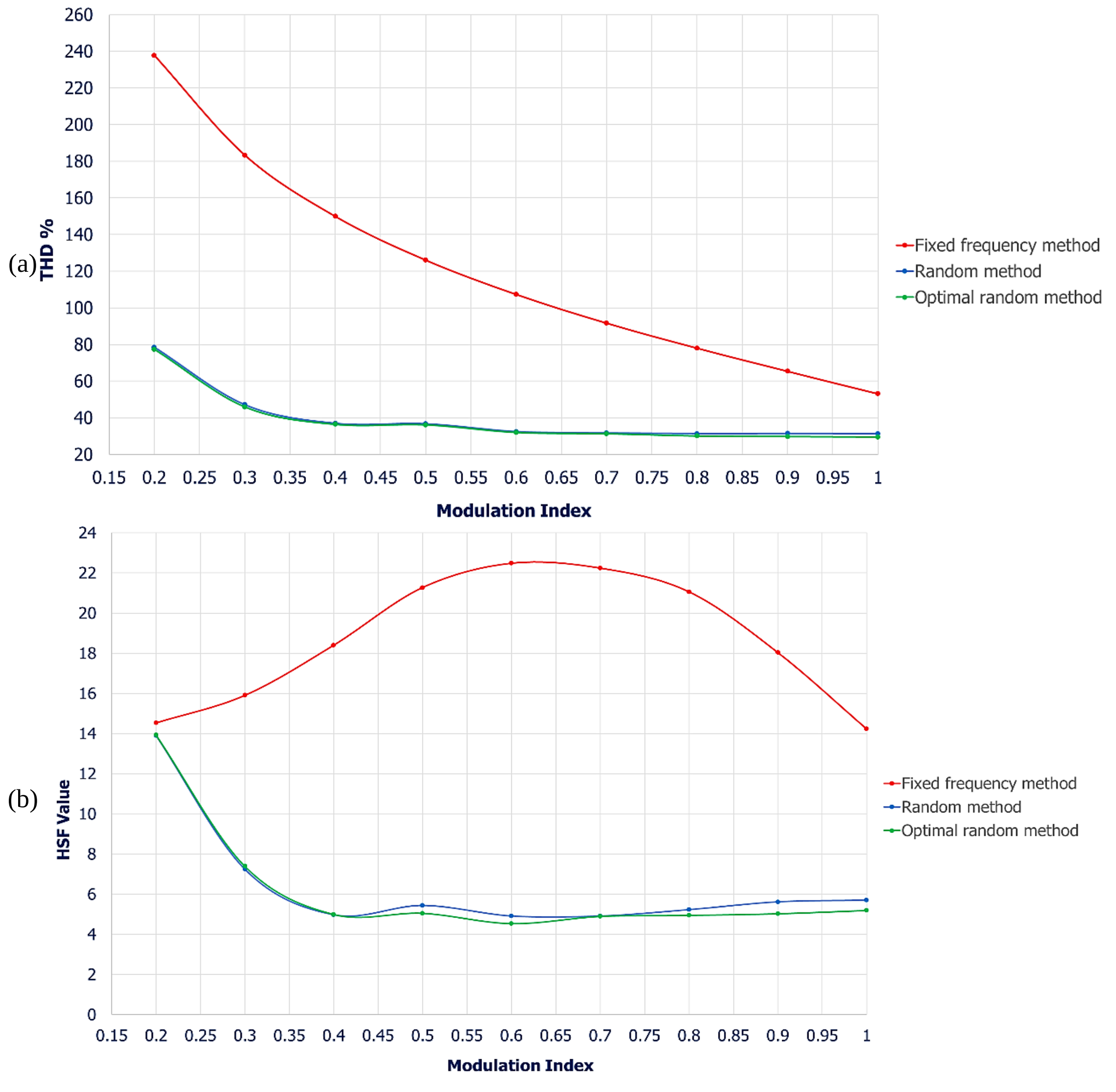

Figure 10. The variation of (a) THD and (b) HSF, as influenced by the modulation index (MI) in option 1

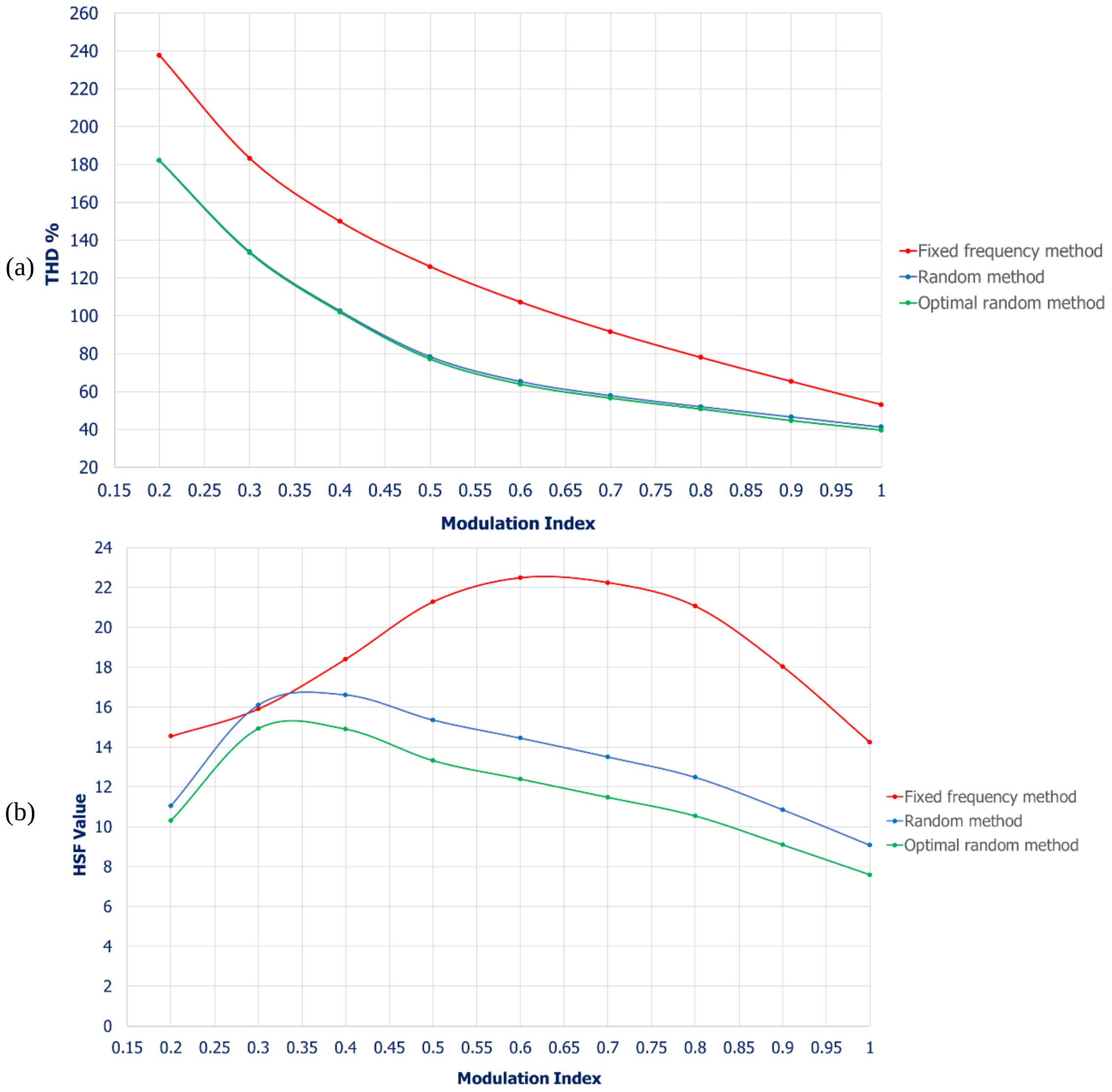

Figure 11. The variation of (a) THD and (b) HSF, as influenced by the modulation index (MI) in option 2

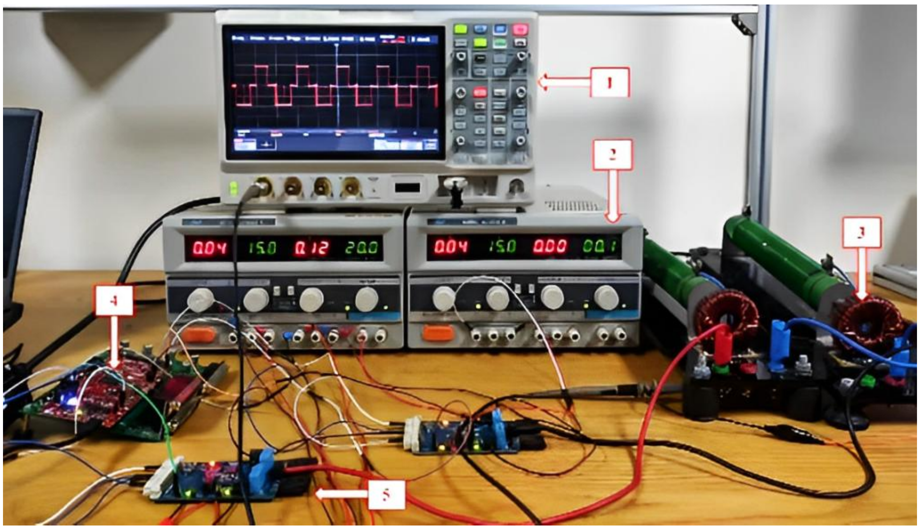

Figure 12. Experimental prototype of the option 1: (1) Oscilloscope; (2) 2× DC regulated power supplies; (3) R-L loads (4 mH, 52 Ω); (4) LAUNCHXL-F28379D; (5) 2× EVAL-1EDI60I12AF modules

A laptop is used for embedded programming with the GA-optimized RPWM algorithm on Code Composer Studio (CCS) to load into the LAUNCHXL-F28379D kit with a sampling time of 4e-5 seconds. Each of two EVAL-1EDI60I12AF modules constitutes a IGBT half-bridge integrated gate driver circuit and by combining these modules, a H-bridge VSI configuration is established. The QJ-3005S III three-way output DC provides a 15 VDC voltage to generate the gate drive voltage for the IGBTs of the 1EDI60I12AF modules and supplies a 20 VDC voltage for modulating the output voltage via the V+HV and GND_HV pins. The output voltage of the two 1EDI60I12AF modules is supplied to the R-L load via two HB_OUT ports. In addition, the SIGLENT SDS2104X plus 4 channel digital super phosphor oscilloscope is employed for the purpose of observing and analyzing the output voltage signal.

The experimental results analyzed by oscilloscope for the harmonic quality of the output voltage on the load (according to method 1) of the optimal sequence and the sequence with the equivalent real-coded value of 65027 are respectively shown in Figures 13 and 14. Figure 15 (see Appendices) shows the simulation results of Harmonic spectrums in logarithmic scale on PLECS to compare with the experimental results obtained on the previously mentioned hardware. Thus, the harmonic spectrum obtained from the experimental results closely matches the simulation results on PLECS software. This demonstrates the effectiveness in harmonic quality with low acoustic noise of the output voltage of the proposed GA-optimized RPWM method.

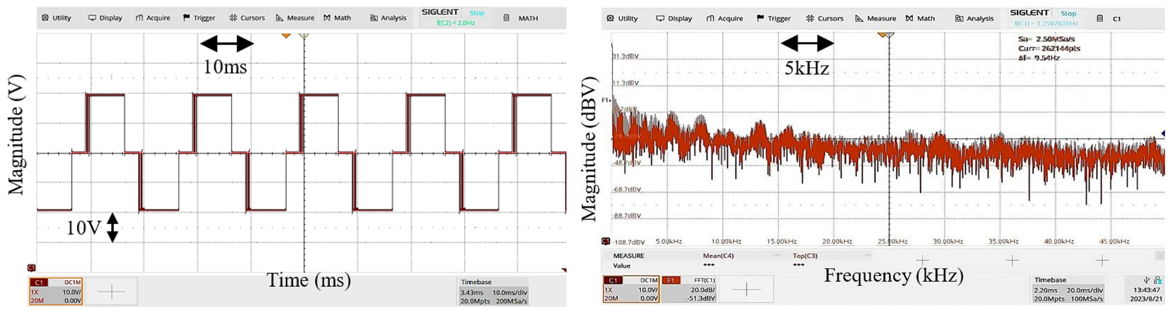

(a) (b)

Figure 13. The output voltage waveform corresponds to the (a) optimal sequence and (b) harmonic spectrum

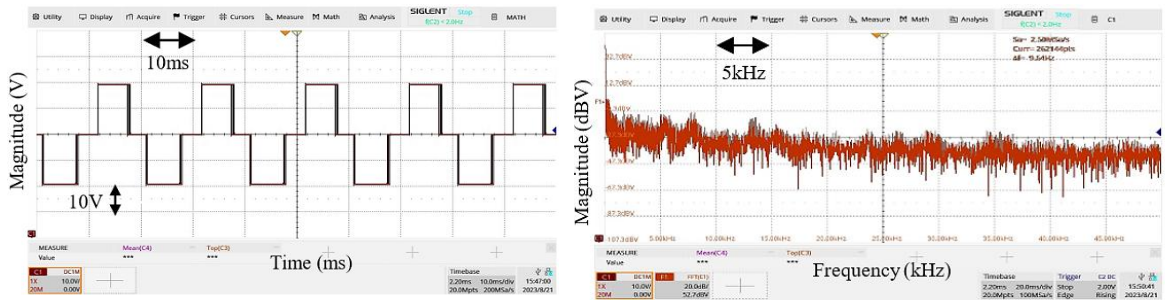

(a) (b)

Figure 14. The output voltage waveform with a modulation index of 0.8 corresponds to the sequence with (a) the equivalent real-coded value of 65027 and (b) harmonic spectrum in logarithmic scale

5. CONCLUSION

In this research, the development methodology for selecting carrier structures using the RPWM technique is proposed. Specifically, a 16-bit binary sequence is employed, and GA are applied to determine the optimal modulation solution. Our approach has been empirically validated and demonstrated to be both effective and feasible. GA-optimized RPWM demonstrates a reduction in THD compared to conventional RPWM. Additionally, GA-optimized RPWM achieves better HSF, leading to effective mitigation of acoustic noise during the operation of systems. Among the two options considered, option 1 emerges as superior due to its absence of dominant harmonics in the high-frequency region. Furthermore, the output voltage waveform of the option 1 demonstrates horizontal axis symmetry, ensuring that the 0th order harmonic is negligible in the harmonic spectrum. Based on the experimental results, GA-optimized RPWM is very suitable to be applied to future renewable energy models, especially the model of self-consumption of PV renewable energy for domestic use.

APPENDICES

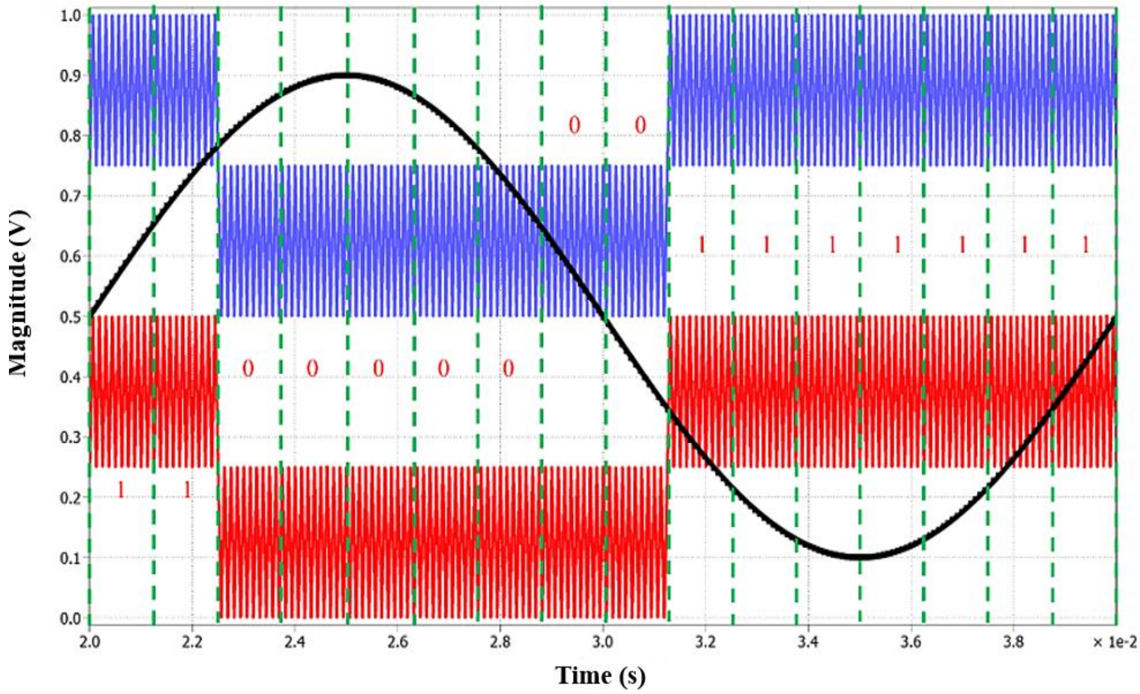

Figure 1. The reference sinusoidal waveform and the carrier waveform delineated by the binary sequence 1111 1110 0000 0011 in the option 1

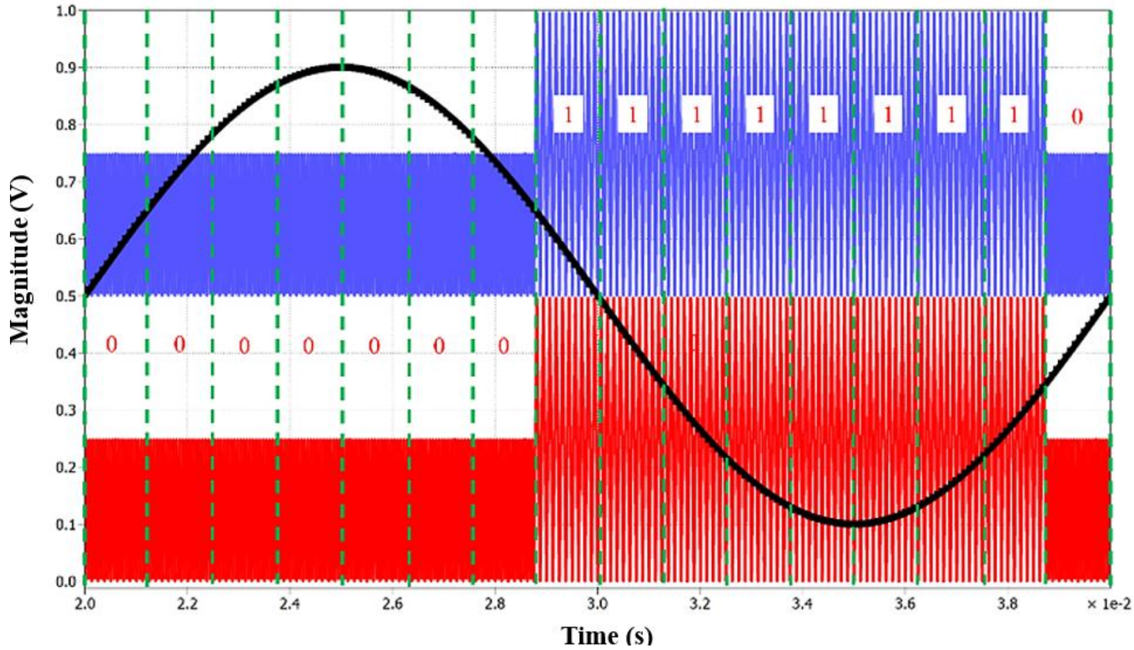

Figure 2. The reference sinusoidal waveform and the carrier waveform delineated by the binary sequence 0111 1111 1000 0000 in the option 2

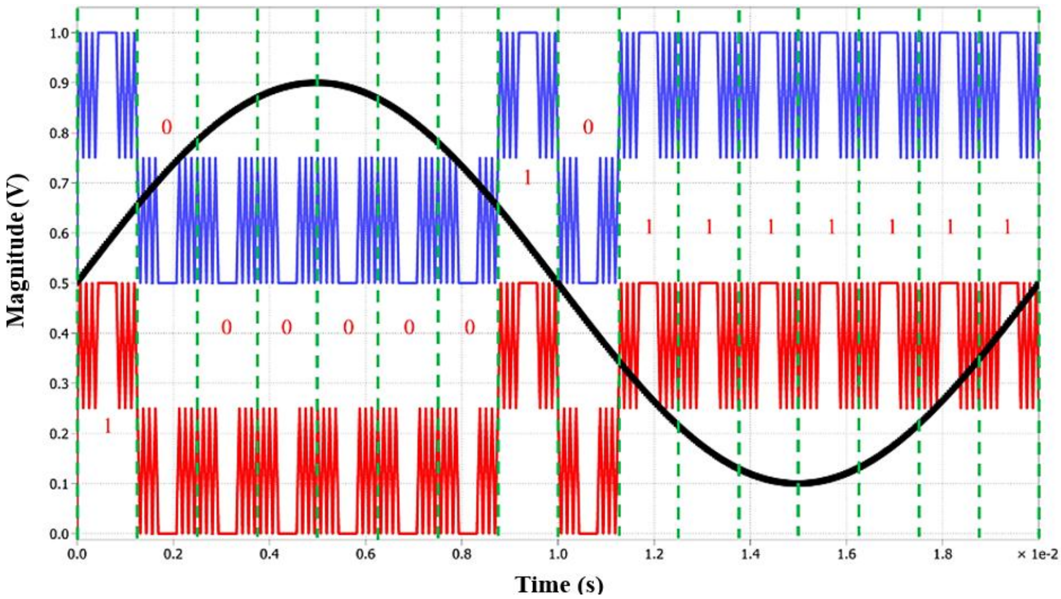

Figure 3. The reference sinusoidal waveform and the carrier waveform delineated by the binary sequence 1111 1110 1000 0001 in the proposal idea

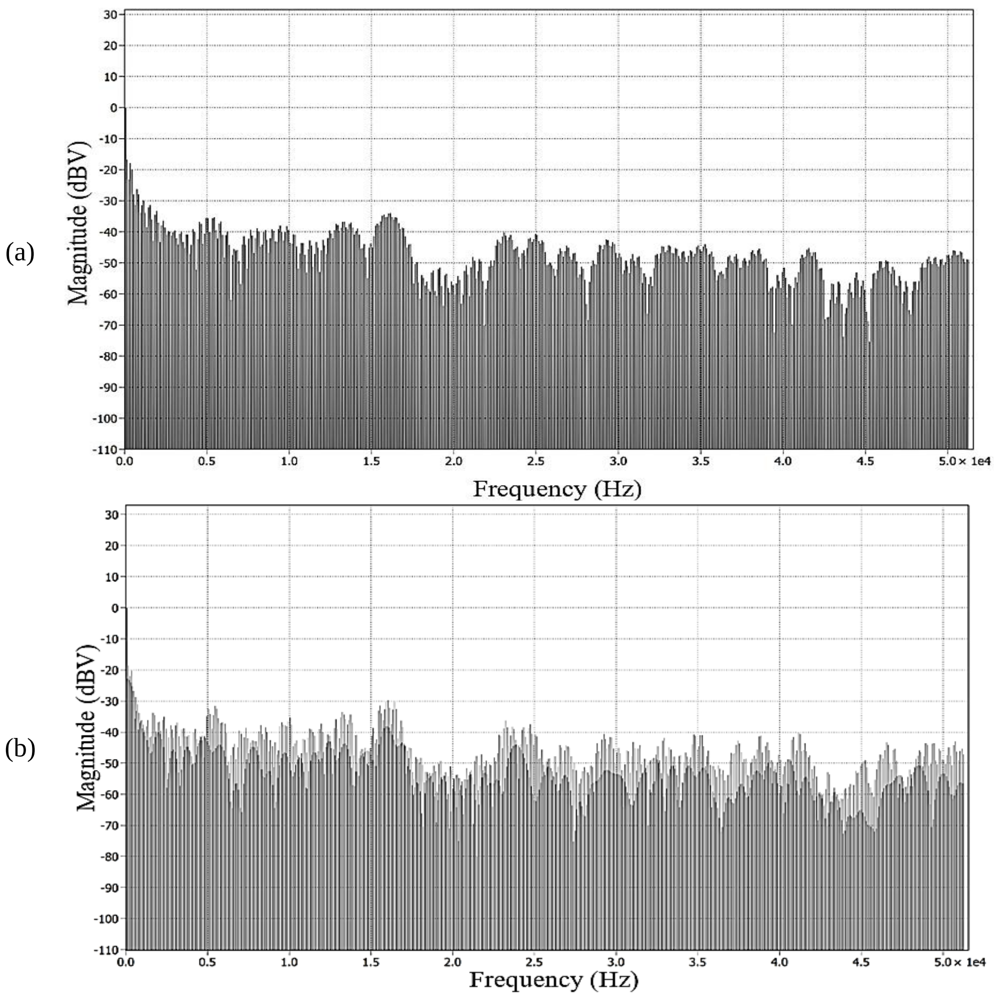

Figure 15. Harmonic spectrums on PLECS software in logarithmic scale correspond to (a) the optimal sequence and (b) the sequence with the equivalent real-coded value of 65027

ACKNOWLEDGEMENTS

We acknowledge the support of time and facilities from Ho Chi Minh City University of Technology (HCMUT), VNU-HCM for this study.

REFERENCES

[1] C. Soumya and T. Jarin, “A novel random carrier frequency modulation technique for drive applications,” *Asian Journal of Applied Science and Technology (AJAST) (Open Access Quarterly International Journal*, vol. 1, no. 9, pp. 526–533, 2017.
[2] R. Jadeja, A. D. Ved, S. K. Chauhan, and T. Trivedi, “A random carrier frequency PWM technique with a narrowband for a grid-connected solar inverter,” *Electrical Engineering*, vol. 102, no. 3, pp. 1755–1767, Sep. 2020, doi: 10.1007/s00202-020-00989-6.
[3] S. N. Lavanya, T. B. Reddy, and M. V. Kumar, “Performance of random PWM techniques for induction motor drive,” *International Journal of Engineering and Advanced Technology*, vol. 8, no. 2, pp. 133–139, 2019.
[4] M. Nayeemuddin, T. B. Reddy, and M. V. Kumar, “Level Shifted Discontinuous PWM algorithms to minimize common mode voltage for cascaded multilevel inverter fed induction motor drive,” *International Journal of Power Electronics and Drive Systems (IJPEDS)*, vol. 9, no. 2, p. 504, Jun. 2018, doi: 10.11591/ijpeds.v9.i2.pp504-518.
[5] J. Xu, Z.-L. Nie, and J.-J. Zhu, “An optimal random carrier pulse width modulation technique based on a genetic algorithm,” *Journal of Power Electronics*, vol. 17, no. 2, pp. 380–388, Mar. 2017, doi: 10.6113/JPE.2017.17.2.380.
[6] J. M. S and K. T. S, “A review on harmonic reduction with random PWM technique for multilevel inverters,” *Global Journal of Engineering Science and Researches*, no. 3, pp. 57–63, 2017.
[7] H. Attia, H. S. Che, T. K. S. Freddy, and A. Elkhateb, “Bipolar and unipolar schemes for confined band variable switching frequency PWM based inverter,” *International Journal of Electrical and Computer Engineering (IJECE)*, vol. 11, no. 5, p. 3763, Oct. 2021, doi: 10.11591/ijece.v11i5.pp3763-3771.
[8] K. T. S, B. A, and K. N. Pavithran, “A comparative exploration on random PWM schemes to spread harmonics for multilevel power converters using cascaded H-bridge configuration,” *International Journal of Applied Engineering Research*, vol. 13, pp. 15696–15700, 2018.
[9] P. A. Kumar and N. P. Subramaniam, “Chaotic triangular carrier based non-deterministic SPWM Strategy for voltage source inverter drives,” *Indian Journal of Science and Technology*, vol. 8, no. 9, p. 842, May 2015, doi: 10.17485/ijst/2015/v8i9/60075.
[10] P. Madasamy *et al.*, “Hybrid multicarrier random space vector PWM for the mitigation of acoustic noise,” *Electronics (Basel)*, vol. 10, no. 12, p. 1483, Jun. 2021, doi: 10.3390/electronics10121483.
[11] D. S. George and G. Shiny, “Random pulse width modulation technique for a 4-level inverter,” *International Journal of Advanced Research in Engineering and Technology (IJARET)*, vol. 6, no. 4, 2015.
[12] G. Chen, K. Li, D. Guo, J. Kang, and C. Ren, “Study on harmonic suppressing performance of random space vector PWM in electric vehicle,” *International Journal of Mechatronics and Applied Mechanics*, vol. 2023, no. 13, pp. 167–173, 2023, doi: 10.17683/ijomam/issue13.20.
[13] G. Chen, Z. Wu, Y. Zhu, and J. Zhao, “Simulation and analysis of random switching frequency space vector pulse width modulation,” *Information Technology Journal*, vol. 12, no. 10, pp. 2009–2015, May 2013, doi: 10.3923/itj.2013.2009.2015.
[14] M. A. Hannan, J. A. Ali, A. Mohamed, and M. N. Uddin, “A random forest regression based space vector PWM inverter controller for the induction motor drive,” *IEEE Transactions on Industrial Electronics*, vol. 64, no. 4, pp. 2689–2699, Apr. 2017, doi: 10.1109/TIE.2016.2631121.
[15] R. G. Kishore and D. T. Udhayakumar, “A random PWM with constant common-mode voltage for PV inverter,” *IJSTE - International Journal of Science Technology & Engineering*, vol. 2, no. 10, 2016.
[16] S. Katoch, S. S. Chauhan, and V. Kumar, “A review on genetic algorithm: past, present, and future,” *Multimed Tools Appl*, vol. 80, no. 5, pp. 8091–8126, Feb. 2021, doi: 10.1007/s11042-020-10139-6.
[17] I. Bukhori, J. Felix, and S. Ali, “Using genetic algorithm to solve puzzle games: A review,” *Journal of Computer Networks, Architecture and High Performance Computing*, vol. 6, no. 1, pp. 201–211, Jan. 2024, doi: 10.47709/cnahpc.v6i1.3348.
[18] J. Li, C. Shang, and M. Zou, “Parameter optimization of linear quadratic controller based on genetic algorithm,” *Tsinghua Science & Technology*, vol. 12, no. S1, pp. 208–211, Jul. 2007, doi: 10.1016/S1007-0214(07)70111-6.
[19] J. Bean, “Genetic algorithms and random keys for sequencing and optimization,” *ORSA Journal on Computing*, vol. 6, no. 2, pp. 154–160, May 1994, doi: 10.1287/ijoc.6.2.154.
[20] X. Xiao-Jie and C. Rui-Min, “Bee evolution genetic algorithm based on real calculations,” in *2012 International Conference on Industrial Control and Electronics Engineering*, IEEE, Aug. 2012, pp. 1938–1940, doi: 10.1109/ICICEE.2012.515.
[21] B. Alhijawi and A. Awajan, “Genetic algorithms: Theory, genetic operators, solutions, and applications,” *Evolutionary Intelligence*, vol. 17, no. 3, pp. 1245–1256, Jun. 2024, doi: 10.1007/s12065-023-00822-6.
[22] J. E. Baker, “Adaptive selection methods for genetic algorithms,” in *Proceedings of the 1st International Conference on Genetic Algorithms*, 1985, pp. 101–111.
[23] B. Burlacu, K. Yang, and M. Affenzeller, “Population diversity and inheritance in genetic programming for symbolic regression,” *Nat Comput*, vol. 23, no. 3, pp. 531–566, Sep. 2024, doi: 10.1007/s11047-022-09934-x.
[24] M. Bogdanović, “On some basic concepts of genetic algorithms as a meta-heuristic method for solving of optimization problems,” *Journal of Software Engineering and Applications*, vol. 04, no. 08, pp. 482–486, 2011, doi: 10.4236/jsea.2011.48055.
[25] J. Nocedal and S. J. Wright, *Numerical optimization*. in Springer Series in Operations Research and Financial Engineering, Springer New York, 2006. doi: 10.1201/b19115-11.
[26] D. Yashesh, K. Deb, and S. Bandaru, “Non-uniform mapping in real-coded genetic algorithms,” in *2014 IEEE Congress on Evolutionary Computation (CEC)*, IEEE, Jul. 2014, pp. 2237–2244, doi: 10.1109/CEC.2014.6900621.
[27] U. A.J. and S. P.D., “Crossover operators in genetic algorithms: A review,” *ICTACT Journal on Soft Computing*, vol. 06, no. 01, pp. 1083–1092, Oct. 2015, doi: 10.21917/ijsc.2015.0150.
[28] F. Rabee and Z. M. Hussain, “Oriented crossover in genetic algorithms for computer networks optimization,” *Information*, vol. 14, no. 5, p. 276, May 2023, doi: 10.3390/info14050276.
[29] F. Herrera, M. Lozano, E. Pérez, A. M. Sánchez, and P. Villar, “Multiple crossover per couple with selection of the two best offspring: An experimental study with the BLX-α crossover operator for real-coded genetic algorithms,” 2002, pp. 392–401, doi: 10.1007/3-540-36131-6_40.

BIOGRAPHIES OF AUTHORS

Quoc Dat Luong is a student studying for an electrical engineering degree at Ho Chi Minh City University of Technology (HCMUT) in the energy systems major since 2019. He is also pursuing a double engineering degree in Electronics and Electrical Engineering at ENSEEIHT, Toulouse INP, France since 2023. His research interests include the field of power electronics, motor drives, industrial electronics, photovoltaic power systems, artificial intelligence, intelligent control, and digital design. He can be contacted at email: dat.luong200190@hcmut.edu.vn.

Manh Duc Nguyen is a student studying for an electrical engineering degree at Ho Chi Minh City University of Technology (HCMUT) in the energy systems major since 2019. He is also pursuing a double engineering degree in embedded systems (EIS) at ESISAR, Grenoble INP - UGA, France since 2023. His research interests include the field of power electronics, automation, intelligent control, embedded systems, and renewable energy. He can be contacted at email: duc.nguyen050901@hcmut.edu.vn.

Minh Khoi Huynh is a drone engineer in the Drone Control Department at MiSmart JSC, Vietnam. He received the B.Eng. degree in Control Engineering and Automation from Ho Chi Minh City University of Technology – VNUHCM in 2024. He has been working as a drone engineer since 05/2022 (at the Drone Control Department of MiSmart JSC, Vietnam, until 01/2024). His research interests include the field of robotics, digital design, sensor fusion, control theory, embedded systems, and unmanned vehicles. He can be contacted at email: khoi.huynh.sophus@gmail.com.

Phu Cong Nguyen was born in Ho Chi Minh City, Vietnam, on March 28, 1983. He is currently working at the Department of Electrical and Electronics Engineering, Ho Chi Minh City University of Industry and Trade (HUIT). He is currently studying towards the Ph.D. degree at the Faculty of Electrical and Electronics Engineering, Ho Chi Minh City University of Technology (HCMUT), Vietnam National University Ho Chi Minh City. His research interests include power electronics and automatic controls. His current research interests include multilevel and multiphase decentralized power converters. He can be contacted at email: npcong.sdh21@hcmut.edu.vn.

Quoc Dung Phan was born in Saigon (now Ho Chi Minh City), Vietnam, in 1967. He received his Dipl.-Eng. degree in electromechanical engineering from Donetsk Polytechnic Institute, Donetsk City, USSR (now Ukraine), in 1991. He received his Ph.D. degree in engineering sciences from Kyiv Polytechnic Institute, Kyiv City, Ukraine, in 1995. Currently, he is an associate professor in the Faculty of Electrical and Electronics Engineering at Ho Chi Minh City University of Technology (HCMUT), Vietnam National University - Ho Chi Minh City (VNU-HCM), Vietnam. His research interests include power electronics (especially multilevel and multiphase converter topology and control), control of electric machines, wind and solar power systems, artificial intelligence, and smart grid. He can be contacted at email: pqdung@hcmut.edu.vn.